

# Programmable Analog System Benchmarks Leading to Efficient Analog Computation Synthesis

JENNIFER HASLER and CONG HAO, Georgia Institute of Technology, USA

This effort develops the first rich suite of analog and mixed-signal benchmark of various sizes and domains, intended for use with contemporary analog and mixed-signal designs and synthesis tools. Benchmarking enables analog-digital co-design exploration as well as extensive evaluation of analog synthesis tools and the generated analog/mixed-signal circuit or device. The goals of this effort are defining analog computation system benchmarks, developing the required concepts for higher-level analog and mixed-signal tools to utilize these benchmarks, and enabling future automated architectural design space exploration (DSE) to determine the best configurable architecture (e.g., a new FPAA) for a certain family of applications. The benchmarks comprise multiple levels of an acoustic, a vision, a communications, and an analog filter system that must be simultaneously satisfied for a complete system.

CCS Concepts: • Hardware → Hardware-software codesign; Memory and dense storage; Analog and mixed-signal circuit synthesis;

Additional Key Words and Phrases: Analog benchmarks, analog system synthesis, mixed-signal HLS, analog computing

### ACM Reference format:

Jennifer Hasler and Cong Hao. 2024. Programmable Analog System Benchmarks Leading to Eficient Analog Computation Synthesis. *ACM Trans. Reconfig. Technol. Syst.* 17, 1, Article 12 (January 2024), 25 pages. https://doi.org/10.1145/3625298

Benchmarks serve as indicators of the fundamental computations perceived within a specific computing substrate. They allow new designers to envision potential applications of the technology and establish connections to desired user core applications. Benchmarks offer performance comparisons and facilitate optimization of the configurable technologies that embody the given technology. Utilizing multiple benchmarks is essential for implementing a technology on a configurable and programmable platform, ensuring that the technology is not optimized solely for a single problem.

Digital design has always had stable benchmarks. Digital high-performance computing benchmarks historically followed the solution of linear equations (A x = b) such as LINPAC [1] or related matrix operations (e.g., FFT, Neural Networks). Linear equations numerically match well with digital computation's (Figure 1) large initial precision and moderate accumulation of partial results [2]. The resulting extensive digital system and tool benchmarks result in a stable landscape

Authors' address: J. Hasler and C. Hao, Georgia Institute of Technology, Atlanta, Georgia 30332-0250; e-mails: ph67@gatech.edu, callie.hao@gatech.edu.



This work is licensed under a Creative Commons Attribution International 4.0 License.

© 2024 Copyright held by the owner/author(s). 1936-7406/2024/01-ART12 \$15.00 https://doi.org/10.1145/3625298

12:2 J. Hasler and C. Hao

[1, 3–22]. A great collection of design benchmarks aims at evaluating the hardware architecture, e.g., embedded processors, Field-programmable Gate Arrays (FPGAs), Graphic Processing Units (GPUs), and heterogeneous systems; representative examples include MediaBench [4], Rodinia [11], OpenDwarfs [12], SHOC [13], CHO [10], Rosetta [7], ERCBench [23], and Koios [8], which use OpenCL, high-level synthesis (HLS), or C/C++. Such designs cover a wide range of applications, such as arithmetic operations, image processing (encoder, decoder), cryptography (encryption, secure hash algorithms), processors (MIPS, RISC), signal processing (FFT, FIR), merge and sort, graph operations (BFS, DFS, MapReduce), wireless communication (error correction), vector and matrix multiplications, and the most recent machine learning (ML) workloads. In parallel, another category of benchmarks aims at evaluating computer-aided design (CAD) tools, e.g., high-level, logic, and physical synthesis [3, 5, 24, 25], such as CHStone [3] and MachSuite [5] for HLS, VPR benchmark suite for FPGA place and route [25], and EPFL benchmark for logic synthesis and optimization [24]. These digital benchmarks not only extensively evaluate hardware architectures and synthesis tools but also guide hardware-software co-design tradeoffs (e.g., [26–29]).

On the other hand, analog benchmarking has great challenges and has not been fully developed for decades. Analog and mixed-signal computing do not have significant benchmarks resulting from a long history of nearly no theoretical framework for computation for three important reasons. First, the *lack* of automated analog design tools compels most analog designers to heavily rely on graphics-based layout and simulation, demanding extensive manual effort with little generalization. Second, unlike digital design, analog designers must be aware of underlying technology nodes and available analog components. Analog designers often struggle with significant parameter variation, making it dificult to design high-level

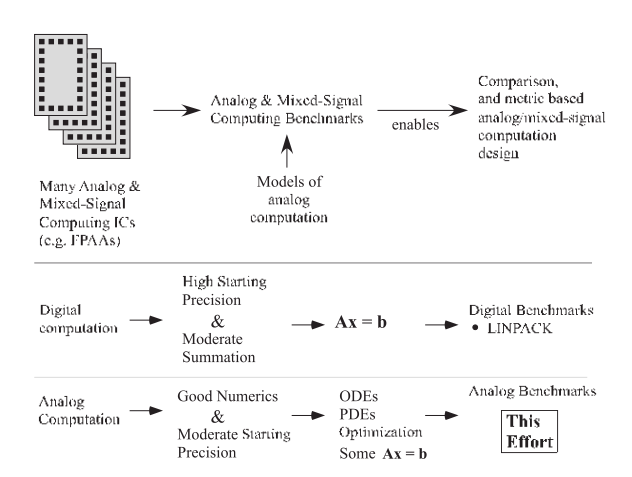


Fig. 1. Development of Analog and Mixed-Signal Benchmarks and resulting metrics. Benchmarks encapsulate what is currently understood of a particular technology.

algorithms that do not expose lower-level analog components to users. Third, while digital benchmarks and circuits can have almost infinite variations by reconfiguring parameters, *analog designs are typically case-by-case*; one reconfiguration (parameter change) may require a whole new design, largely limiting the scalability and generality of benchmarks. Therefore, a representative and rich analog benchmark suite has never been proposed or discussed.

Developments in analog and mixed-signal programmable and configurable systems, such as large-scale Field Programmable Analog Arrays ((FPAA), e.g., [30]) and the SoC FPAAs (Figure 2) [31], provided the opportunity for developing analog computing theory [2, 32–34] and created the need for synthesis tools and benchmarks that guide the tool development. Reconfigurable analog systems, like FPAAs, are a mixture of reprogrammable values that determine network topology as well as computation parameters. These devices have evolved without a set of benchmarks. Analog computing theory has been recently developed [2, 32–34], built on rich user experiences. Now that both the theory and reconfigurable FPAA platforms that implement these concepts are both mature, this article defines the first analog benchmark suite.

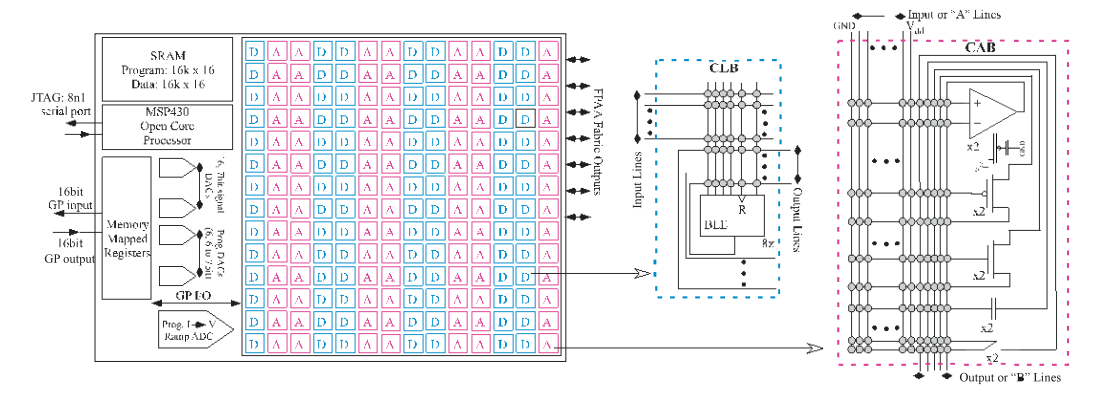


Fig. 2. SoC large-scale FPAA computational blocks and routing architecture. The Computational Analog Blocks (CAB) are typical of earlier CAB designs, being combinations of transistors, OTAs, FG transistors, OTAs, capacitors, T-gates, current mirrors, and signal-by-signal multipliers. The Computational Logic Blocks (CLB) are 8, 4 input Boolean Logic Element (BLE) lookup tables with latch. The SoC FPAA employs an open-source MSP 430 microprocessor ( $\mu$ P) [35] with on-chip structures for 7bit signal DACs, a ramp ADC, memory-mapped General Purpose (GP) IO, and related components.

This discussion aims to address these challenges based on the accumulated expertise in *analog reconfigurable devices* (e.g., [30, 36]) and *programmable circuit designs* (e.g., [37, 38]) by proposing the first representative and reconfigurable analog benchmark suite. The goal is to build an ecosystem of analog design and benchmarking by defining standard benchmark format and scope. This work formally defines the analog benchmark set at different levels, including application, algorithm, and block levels. New analog synthesis tools and hardware benchmark implementations, although currently being developed, will not be discussed as they are beyond the scope of this article. The benchmark definitions can ease the effort of developing future analog synthesis tools by clearly defining the interfaces to analog libraries and by decoupling HLS and low-level (circuit) synthesis. The contributions and significance of this work are summarized as follows.

- This work proposes the first representative and rich set of analog benchmarks that are at different levels of complexity and are expressive with reconfigurable and customizable parameters.
- The proposed *analog benchmarks* arise heavily from analog computation capabilities. Analog benchmarks require understanding the fundamentals of analog computation to abstract circuit details into a meaningful top-down design flow.
- This work discusses the feasibility of the proposed benchmarks, demonstrating that they can
  be synthesized into existing analog circuits, either reconfigurable FPAAs or an integrated
  circuit (IC).

All designs, files, and reported numbers using these benchmarks are openly available. We hope that the defined benchmarks in this work can provide standards for future analog synthesis (compilation) tool development, as well as further analog benchmark development, which requires not only effort from one group but from the entire community.

This discussion first overviews the current state of analog and mixed-signal systems and tools (Section 1). Then the discussion abstracts the capabilities of analog computing (Section 2) to show

<sup>1</sup>https://hasler.ece.gatech.edu/AnalogBenchmarks

12:4 J. Hasler and C. Hao

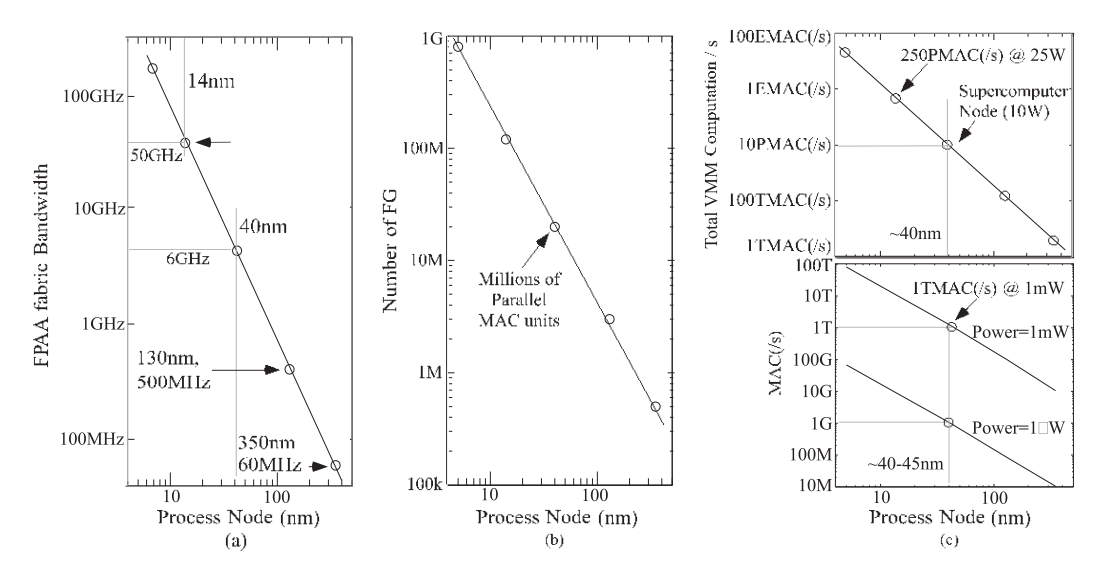


Fig. 3. The potential of scaled down FPAA devices, enabled through synthesis tools, from extrapolations from experimental measurements and early studies of scaled down FG and FPAA devices (350 nm to 5 nm). These opportunities motivate the need for synthesis tools to enable these new devices at commercial timescales. (a) scaling of the resulting fabric computational bandwidth. (b) scaling of available analog FG devices, and, therefore, the number of computational parameters and devices. (c) The computational and computational efficiency opportunities for scaled down  $5 \times 5 \text{ mm}^2$  FPAA devices. Existing FPAA systems (e.g., 350 nm CMOS) enable significant computation ( $\approx 1 \text{TMAC}(/\text{s}), \text{MAC} = \text{Multiply ACcumulate})$  and computation at low energy levels ( 10 GMAC(/s) in 1 mW), scaled down FPAA devices enable embedded supercomputing capabilities in mW power levels.

the resulting analog benchmarks (Section 3). These benchmarks are composed of an initial set of analog and mixed-signal *algorithm* blocks that provide solutions for these particular benchmarks (Section 4). Benchmarking (Section 5) also enables analog-digital co-design exploration and enables automated architectural design space exploration (DSE) to determine the best configurable architecture (e.g., a new FPAA) for a certain family of applications.

### 1 FPAA TECHNOLOGY AND TOOL OVERVIEW

The SoC FPAAs and earlier families of Floating-Gate (FG) enabled FPAAs demonstrated a number of core concepts, as elucidated from early large-scale FPAA techniques in 2002 [39] to today's devices (e.g., [30]). FPAAs have analog components with routing between analog and digital components, similar to FPGAs. Early programmable analog arrays [40–42] and early commercial devices (e.g., EPAC [43] or Anadigm [44]) were useful as *glue* logic and functions and for small occasional computations. Today's fully reconfigurable and nonvolatile FPAAs show considerable capabilities in ultra-low power computation (1,000 × lower than digital [45] following Mead's Hypothesis [46]), signal processing, and embedded ML [30] from ICs fabricated in a 350 nm CMOS process. Programmable analog FG techniques have demonstrated precision components [47] built on work enabling programmable design for temperature [48]. FPAAs have also been integrated with sensors, possibly fabricated on the FPAA fabric [49, 50].

Large-scale programmability is essential for these FPAA devices, typically instantiated using analog-programmable FG devices available in standard CMOS for the memory and routing

elements. Today's SoC FPAA [31] utilizes 600,000 programmable parameters in 350 nm CMOS (Figures 2 and 3). Analog programming of the single FG pFET device fabric enables computation in routing fabric as well as Computational Analog Block (CAB) elements [51]. FG parameters tend to provide a 1,000 × advantage over other Si memory approaches at roughly 8–10 bit level [30]. FG devices have demonstrated long-term (10-year) lifetime across multiple IC processes from 2  $\mu$ m to 40 nm linewidths [47, 52, 53] with precision (e.g., 14-bit) targeted (re)programming of heterogeneous arrangements of FG devices [54]; FG devices enable the direct elimination of mismatches or the setting of desired target values in the configurable structure. FPAA devices are capable of secure operation [55].

From experimental measurements in scaled down processes (e.g., 14 nm or 40 nm, [56]), to-morrow's FPAAs [36] will use parallel operations available in energy-constrained environments (Figure 3), enabling ubiquitous devices for embedded *and* high-performance applications. Programmable techniques have shown promise enabling scaled down analog design, avoiding device mismatch dificulties in scaled process analog IC design [53, 56]. Besides higher density and lower energy consumption, smaller CMOS linewidths (e.g., 40 nm) enable RF frequency signals (e.g., 4 GHz and higher) through FG routing fabric [53]. Current mixed-signal systems and designs are highly restrictive of IC process choices, due to the manual design effort involved when moving to a new IC node but not technical limitations.

The large system size makes design tools essential for FPAA system development, similar to FPGAs, and the development of FPAA devices has been the motivation for the most advanced efforts in analog tool development. FPAA design tool development [57–59] gives users an increased ability to create, model, and simulate analog and digital designs. High-level design tools implemented in Scilab/Xcos can automate the circuit compilation into a *switch list*, the description of the programmed FPAA hardware [57]. These graphical tools correspond to the natural analog dataflow computation, enabling a non-circuits expert, like a system application engineer, to investigate particular algorithms. These tools also enable (Figure 4) system level design and macromodeled simulation (level = 1) and circuit level design (level = 2) [59], including both FPAA targeting and simulation [60]. The chip details are specified in architecture files for the analog-digital SoC FPAA, enabling place and route [61] in a user transparent process.

Synthesis tools can unlock the potential of analog architectures to achieve real-time computation, signal processing, and inference and learning for low SWaP (Size, Weight, and Power) systems in commercial timescales (Figure 3). Empowered by the initial FPAA design and synthesis tools and recent developments for analog and mixed-signal standard cell library formulation and implementation [62, 63], opportunities exist for synthesis from text-based behavioral (e.g., Python) and high-level (e.g., Verilog) abstractions to configurable devices, custom silicon IC layout (.gds), or the

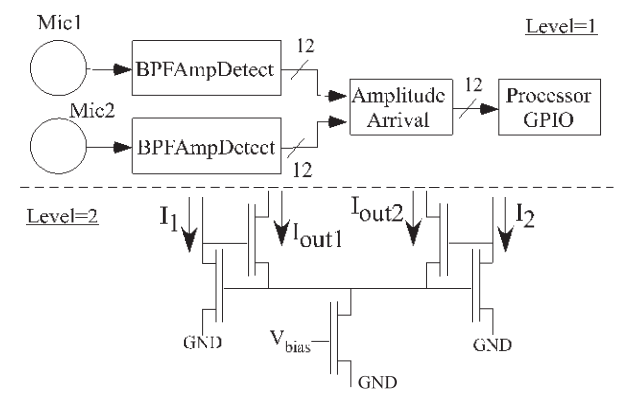


Fig. 4. Review of the two levels of analog abstraction, level = 1 for vectorized, voltage-mode, system level dataflow representations, and level = 2 for full current-voltage analog cell representation used by an analog designer.

12:6 J. Hasler and C. Hao

design of new FPAA devices, as well as macromodeled simulation from these high-level formulations.  $^2$ 

#### 2 BASICS OF ANALOG COMPUTING

Configurable FPAA devices motivate the need for analog and mixed-signal benchmarks in using and evaluating automated synthesis tools. Formulating these benchmarks require understanding the nature of analog computation. The digital VLSI revolution [64] with IC process scaling [65–67] is because of the well-developed digital theoretical foundations [68] and frameworks. However, analog computation largely relies on artistic development, and, therefore, could not directly take advantage of IC process scaling. The following four decades have seen the slow building of analog computing concepts.

The initial FPAA successes made analog computing theory both a practical direction with realistic technology considerations, as well as a necessary development for system design. Analog computation nowadays has far exceeded its early state of a few passive components around some op-amp blocks and goes beyond a few signal conditioning circuits using resistors around an op-amp or a useful component used in digital infrastructure (e.g., PLL). Therefore, widespread programmability is essential for any computing approach and analog component design must avoid being stuck in the artistic space where users need to be developing designs that fit well with the larger system technology.

The development of analog abstraction and the design of modular analog computing components directly come out of the FPAA tool development and enable the opportunities for benchmark systems [32]. The development of analog numerical analysis dispels the belief that analog is an imprecise computing medium compared to pristine digital methods, but rather, digital and analog computations have their own strengths in corresponding areas [2]. The development of analog architectures gives a roadmap for efficient analog computation, showing that communication is the primary cost in analog computing given the local analog computing efficiency, particularly communication with memory components [33]. These three parts enabled the development of a real-valued Turing Machine model for analog computation, providing a theoretical framework for these approaches [34]. The real-valued computation and theoretical modeling reveal the limitations of digital (integer-valued) simulation of analog computation: digital simulation is not, and will not ever, be completely sufficient for analog system design compared to physical system implementations. These concepts begin to make analog computation a top-down design methodology.

Analog Computation. Analog computation directly utilizes Ordinary Differential Equation (ODE) or Partial Differential Equation (PDE) computations in vector or matrix formulations as a result of the ideal summation (enables long summations) and continuous-time (CT) integration properties [2]. Both analog and digital computations compute Vector-Matrix Multiplications (VMM) in an eficient form given their technology framework, where analog VMM tends to be 1,000 × more energy eficient than digital (e.g., [45, 69]). The extension of the dense mesh crossbars of FG elements for VMM computation started the Computing-in-Memory (CIM) efforts in 2001 [38]. ODEs describe CT physical systems, such as electronic circuits, governed by physical laws. The integration of capacitors and currents is a physical law with no inaccuracies [2]; the primary device mismatch is threshold voltage mismatch that is

 $<sup>\</sup>overline{^2}$ Multiple articles are currently in submission, and upon acceptance will be referenced in this section. We are enthusiastic to provide accepted articles to the reviewers.

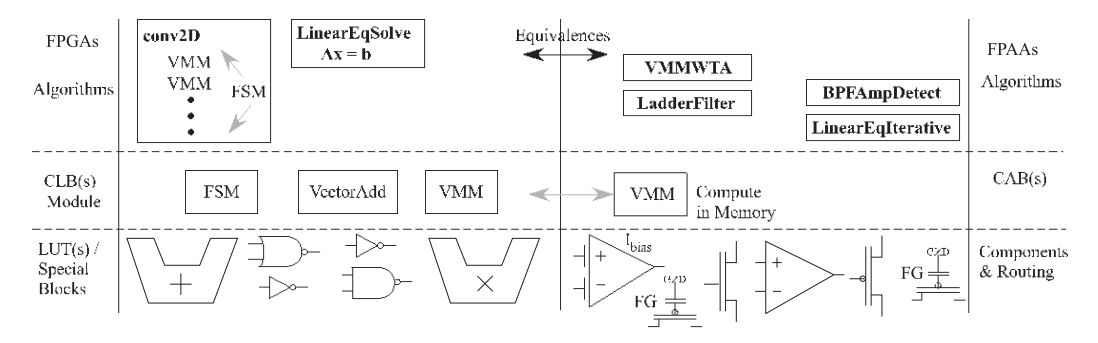


Fig. 5. Parallel FPGA and FPAA Levels of complexity. As FPGAs have algorithms that are composed of modules utilizing one or multiple CLB that in turn utilize fundamental logic gates (e.g., LUTs) and components, FPAAs have algorithms that are composed of blocks utilizing one or multiple CABs that in turn utilize multiple components (e.g., transistors or Transconductance Amplifiers (TA)) or routing elements.

directly addressed through FG programming. While a digital problem usually can be solved by simplifying to A x = b, an analog problem can be solved by simplifying it to a set of ODEs. An analog system can solve systems of linear equations by setting up a differential equation with a steady-stated described by A x = b [70]), although an effective analog L U decomposition still remains an open question. Although the ODEs for these benchmark problems can be digitally simulated, building the full system can enable complete characterization and thus is beneficial.

Analog Abstraction. Analog computation follows a flow-graph representation (e.g., Simulink or Xcos) effectively assuming single-ended voltage-mode busses of signals. The levels of analog components have similar parallels to digital components, where the point of connection and direct comparison is at the algorithm level (Figure 5). These vectorized (Figure 6) signal busses result in efficient high-level graphical representations. These analog system level designs are built from abstracted level = 1 blocks (Figure 4), enabling a dataflow graph of macromodelled single-ended vectorized voltage input and output signals [32, 57, 59]. The capabilities to do classical analog design are continued and enabled through level = 2 blocks that utilize the fullness of the current-voltage implicit functionality of the available devices (Figure 4). These experimentally demonstrated level = 2 devices would be the essential building blocks for new level = 1 devices when fully macromodelled and vectorized. The resulting system in the FPAA or in the resulting structure will require known blocks for control flow and programmable infrastructure components.

Analog Architecture. The proper analog or digital architecture [33] choices directly impact the design of an eficient and high-performance system. For sensor systems, one wants an *end-to-end* computation from analog input signals from a sensor interface to refined digital or near digital classified outputs. Analog computation ideally operates at the speed of the input or output data, since buffering (e.g., memories) is expensive due to the communication cost. Effectively, the computation becomes free and communication is the primary issue, arguing for co-located memory and computation. Other approaches, such as using an analog computation as a specialized routine (or co-processor) to a main digital system, often are a mismatch to the technology (e.g., requiring many DACs and ADCs at the boundary), to the numerics, as well as to the targeted application problem (e.g., Mythic Semi [71]).

12:8 J. Hasler and C. Hao

#### 3 DEFINITION OF ANALOG BENCHMARKS

The proposed benchmark suite addresses a wide range of analog and mixed-signal computations (Figure 7). The development of programmable and configurable systems, whether digital or analog, requires multiple benchmarks not to optimize for a single computation but to enable wide applicability of the technology. This benchmark suite could also be solved using digital computation when including the necessary data converters, providing useful comparisons between digital and analog designs and eventually co-design opportunities.

Analog benchmarks must consider a wide range of analog computations from sensor signals, such as sound, image, or communication. Benchmarks are end-to-end definitions from sensors to refined computation output, providing a fair comparison of analog computing approaches with other technologies. Figure 7 gives an overview of our proposed benchmarks spanning a wide application range with different parameters and sizes (Case I to Case IV). There is one significant bench-

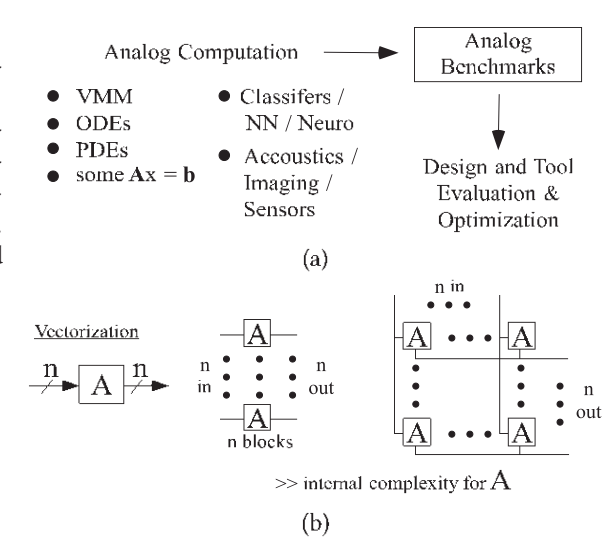


Fig. 6. Development of Analog and Mixed-Signal Benchmarks and resulting metrics. (a) Benchmarks encapsulate what is currently understood of a particular technology. Analog Benchmarks build from the advantageous analog computations. (b) Analog abstraction requires encapsulating analog computations into a dataflow framework, requiring a range of vectorized analog components.

mark in speech processing for acoustic processing (Section 3.1), one significant traditional analog system design (a 10<sup>th</sup> order programmable CT *filter*, Section 3.4), one significant benchmark in vision that includes image classification (Section 3.2), and one significant benchmark in communications (e.g., RF) computation (Section 3.3). Two of these benchmarks (acoustic and vision) utilize embedded ML as part of their operation. The communication benchmark likely will use ML, and the filter benchmark could be framed as an optimization problem solved through ML. The labeled training and testing set applied to the sensor input specifies the benchmark inputs and outputs. Part of the benchmark examples requires training the benchmark parameters for the analog implementation. The training can be done either off-line or on-the-fly on the physical system; on-chip learning has already been demonstrated for analog computation, including configurable FPAA systems [72, 73]. One expects further benchmarks to be defined along these directions.

These benchmarks (Case I to Case IV) are designed for multiple problem sizes (Figure 7) to illustrate as well as normalize between different IC technology nodes. One might find certain problem sizes that are not achievable by a 350 nm CMOS IC process, and yet might be achieved by a 130 nm, 40 nm, or 14 nm CMOS IC process. Reconfigurable applications directly connect to the roadmap of what can be built in different CMOS linewidths, and the proposed benchmarks provide system-level computational comparisons. All four benchmarks in a given case must be created and characterized when evaluating a reconfigurable platform or analog synthesis tool. Cases I through IV vary in levels of dificulty and complexity, showing different capabilities for a system satisfying all four benchmarks. For example, the SoC FPAA (350 nm CMOS) would handle the Case

		Case I		Case II		Case III		Case IV	
	Computation	Size	Freq	Size	Freq	Size	Freq	Size	Freq
Acoustic	Command / Speech recognition								
	from microphone signal:	$4^{a}$	$20 \mathrm{kHz}$	32 <sup>b</sup>	$20 \mathrm{kHz}$	256	$20 \mathrm{kHz}$	1000	20kHz
Vision	Image Classification	$MNIST^c$	60fps	$MNIST^d$	60fps	$1 \mathrm{Mpixel}^{e}$	60fps	$10 \mathrm{Mpixel}^{e}$	60fps
Comm	Beamforming and								
	Demodulation (0.01× input freq)	8	3MHz	16	50MHz	32	2GHz	64	20GHz
Filter	$10^{th}$ Order Programmable LPF	1	300kHz	1	3MHz	1	30MHz	1	300MHz

<sup>a</sup>Command Word Classification, <sup>b</sup>Small Vocabulary Classification

Fig. 7. Creating the first Analog and Mixed-Signal Benchmarks. Defining the first benchmarks for analog and mixed-signal computation requires encapsulating core analog computations. Analog computation centers around solving differential equations using sensor inputs. These starting benchmarks can have additional benchmarks added as technology continues to grow.

I benchmarks (e.g., [31, 73–75]), while further improvements could address some of the Case II benchmarks. Scaled CMOS processes (e.g., 40 nm CMOS) are capable of reaching the Case III and Case IV benchmarks (e.g., [53], Figure 3). Potentially, benchmarks in more complicated cases (e.g., Case V) can be defined on top of the success of earlier benchmarks. The important benchmark measurements would be energy and/or power consumption, accuracy, and the area or resource utilization for the computation. Another measurement (Imager Benchmark) identifies the amount of required non-local communication, as well as intermediate memory storage, to minimize architectural costs when operating at the input (sensor-driven) and output (classification/computation). Each benchmark uniquely stresses the analog programming capability of the resulting analog system. The particular physical solution will depend on the available sensors (e.g., types of imagers, types of microphones) to the engineers.

Analog circuit problems outside of these computing spaces would not make good benchmarks, because they are often highly specialized analog design questions. For example, level-shifting (e.g., voltage) amplifiers that are often solved through specialized technologies (e.g., 100 V supply GaN amplifiers) are not a useful benchmark; when needed, such devices can be integrated into modules with a programmable device. Similarly, specialized sensor interface blocks or data converters might be used in a benchmark system but are not considered as a benchmark. Other traditional analog circuit blocks that assist in digital systems, such as Phase Locked Loops (PLL), are typically blocks in a larger system (e.g., a standard-cell block), and thus are not a full benchmark either. Analog computation benchmarks should focus on larger analog computing capabilities.

### 3.1 Acoustic Benchmark: Microphone to Word Classification

The first benchmark is a programmable end-to-end microphone-to-symbol keyword/word/ acoustic symbol classifier. The input bandwidth is 20 kHz for all problems, set by the input microphone sensors in the range of human hearing. Existing solutions use a filterbank of incoming signals in a near exponential spacing of center frequencies (e.g., 50 Hz to 10 kHz) that model the human cochlea dynamics (e.g., [31], preserving the highest signal and frequency information while refining the data representation. Current solutions might take the raw microphone input through a set of programmable parallel bandpass filters (16–24) followed by an amplitude detection (Figure 8). The amplitude detection produces a set of analog signals indicating a filtered magnitude of a set of frequencies. Some existing solutions implement additional dynamics or approximate delays [75] before or in the classifier. Programmability enables repeatable front-end computing structures by eliminating the effect of mismatch, resulting in a near-ideal transfer function for each filter channel.

<sup>&</sup>quot;Compressed DCT, 19-8-6-4 NN, d3-layer NN, "Image convolution / classification

12:10 J. Hasler and C. Hao

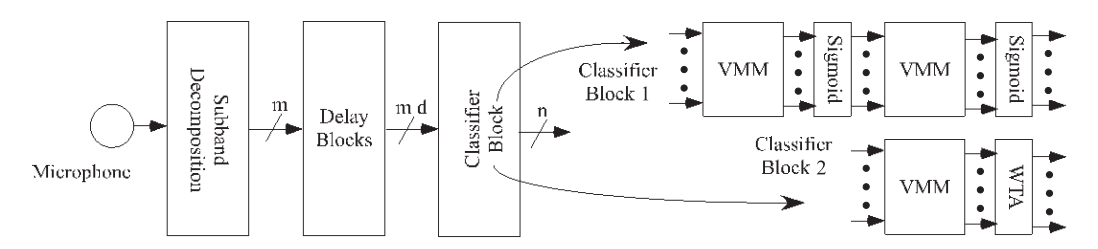
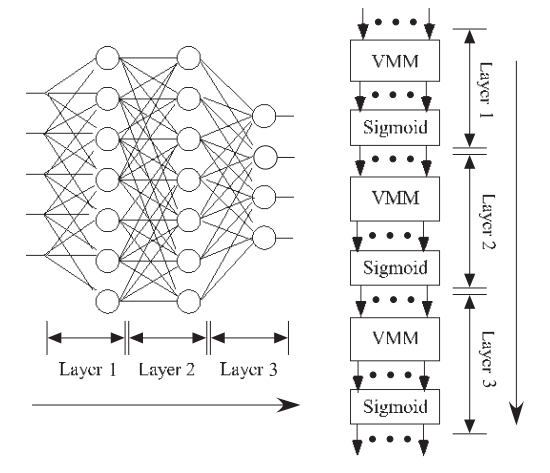


Fig. 8. Benchmark circuit for the command-word recognition benchmark (acoustic). Multiple existing physical implementations for the classifier block would include a VMM+WTA universal approximator classifier.

This benchmark classifies the sound signal representations into words or other acoustic symbols (Figure 8). Typical implementations of such classifiers use a feedforward computation, although recurrent architecture might present significant performance improvement for different vocabularies with little additional system cost to implement the resulting ODEs. The classifier (Figure 8) could be implemented as a multi-layer neural network (NN) (Figure 9), or one or multiple layers comprised of VMM + a Winner-Take-All (WTA) universal approximator/classifier. The quality of the programmability available for an experimental solution will directly impact the measured metrics to



this benchmark. The output is a binary digi- Fig. 9. Embedded NNs are essential for most of the tal classification, or a low-bit (2–4bit, straight- benchmark problems, where a number of potential arforward ADC) sparse representation that gives chitectures utilizing one to multiple layers might be a confidence measure for the identified words.

The sparse output has a low sample rate for the

next system (e.g., 1–10 samples/s) that likely would be event encoded. The classified vocabulary size (Case I: 4 Case II: 32 Case III: 128 Case IV: 1,000) shows the system classification capability. The labeled input datasets for this benchmark are

- Case I: 4 words from TIMIT [76] or TI digits database [77].
- Case II: Speech Commands Dataset [78]: 32 labeled words from multiple (5) speakers (made available through Google).
- Case III: 128 words from the labeled dataset LibriSpeech [79] (similar sized datasets are possible).
- Case IV: 1,000 words from the labeled dataset LibriSpeech (similar-sized datasets are possible).

One can find openly available versions of all these datasets. Forms of this benchmark (primarily Case I) have been demonstrated within configurable platforms [31, 73, 80]. As one might only be able to obtain a microphone with an LNA, any reported result must describe if the system uses a raw microphone or microphone with LNA as well as the input signal SNR levels. The classified output is defined through the labeled dataset. The users of a particular dataset will have to train their network for the particular dataset, e.g., through ofline training. If users have technology capable of on-platform training, that should also be identified with the resulting energy eficiency

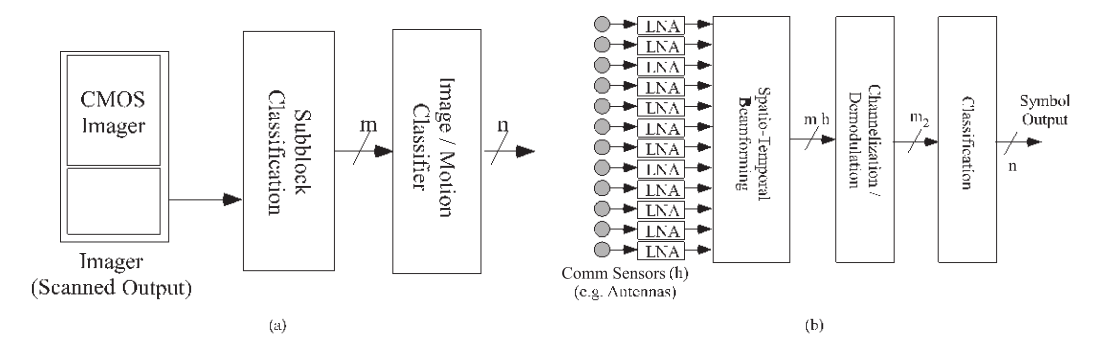


Fig. 10. The vision and communication Benchmark circuits. (a) Vision benchmark circuit. (b) Communication benchmark circuit.

of the training. Metrics for this benchmark include energy eficiency, accuracy of classification starting from sensor input, and area of the resulting system.

# 3.2 Vision Benchmark: CMOS Imager to Classification

The large number (e.g., millions) of pixel sensors for vision classification challenges the analog computational and communication complexity. The size of the image classification problem becomes the primary parameter, where the frame rate tends to be nearly fixed for most applications looking for human-like performance. The classifier should operate at the input signal rate. The system must start from a commercially available (e.g., production or R&D moving to production) CMOS imager requiring an input signal that is a two-dimensional scan of the image plane or an event representation of the image plane (Figure 10). This communication bottleneck significantly constrains the computing architecture as one must minimize the movement of data into short-term storage [33]. Many computations utilizing two-dimensional representations experience similar issues. Commercial imagers have either digital or analog datapath out of the imager; having either input signal into the analog processing is reasonable, even if an initial DAC is required to recover the single analog signal. Communication from the imager is part of the benchmark measurements. An imager die stacked on a configurable analog structure enables a number of different computational opportunities [36], although often with significant additional cost. The first two vision processing Cases (I and II) are static image classification (Figure 9). The last two vision processing Cases involve both image classification as well as motion processing (changes between images), utilizing recurrence and dynamics in analog computation. The particular classifier builds up representations (Figure 9), starting from symbols from initial local image refinement for the larger image processing. The input would need to be projected on an imager module that must be large enough for the entire image and then processed for the full benchmark problem to the classified outputs. Identifying the imager device (e.g., commercial product, event imager, specially built device) allows for comparison of the resulting algorithm. The labeled datasets form the inputs and resulting desired outputs for the benchmark; the labeled datasets would be:

- Case I and II: MNIST image dataset [81].
- Case II: COCO 2017 dataset [82], the dataset used in the ResNet [83] classification models.
- Case III and IV: SVD Video labeled dataset [84].

A particular labeled dataset requires training the physical computing system for that dataset as classifier implementations are design dependent. Metrics for this benchmark include energy eficiency (continuous-image classification), accuracy of classification starting from sensor input, and area of the resulting system.

12:12 J. Hasler and C. Hao

## 3.3 Communication Benchmark: Beamforming and Classification

The communication benchmark is a common module for RF-based communication systems from sensors (e.g., Antenna structure) through classified output. Fundamental computations include spatio-temporal filtering for beamforming and frequency shaping (e.g., equalization) and filtering, potential channelization (linearly spaced bandpass filters), demodulation, and classification of the resulting complex baseband signals. The spatio-temporal filtering requires approximate delay lines or similar decompositions and a VMM (e.g., [75]). Symbol classification (Figure 9) includes identifying the complex transmitted value in say a QAM64 or higher standard. The cases are scaled by center bandwidth frequency, as a higher operating frequency significantly increases the system complexity (Case I: 3 MHz Case II: 50 MHz Case III: 2 GHz Case IV: 20 GHz). The cases are scaled by the number of input signals for a single element for the front-end spatio-temporal filtering (Case I: 8 Case II: 16 Case III: 32 Case IV: 64). The resulting demodulated output then gets classified into symbols. The number of labeled communication (e.g., RF) datasets is limited, although a few exist (e.g., [85]) to be used for this measurement. It is assumed that the output signals would be coming out of a communication source (e.g., Antenna + LNA) and should be identified. Metrics for this benchmark include energy eficiency, accuracy of classification starting from multiple voltage-signal inputs, and area of the resulting system.

# 3.4 Analog Benchmark: Low Power, High-SNR Programmable Filtering

The analog computation functions are balanced by a traditional analog computation problem of a programmable low-power and high SNR  $10^{th}$ -order Low-Pass Filter (LPF). A BPF is already addressed through the acoustic benchmark, therefore, this effort focuses on programmable LPF filters. Existing solutions typically utilize a cascade of  $2^{nd}$ -order programmable filter blocks [86] or a programmable ladder filter block [75]. This benchmark would be measured by the consumed resources/area, circuit power, and achieved SNR. This benchmark will stress the programming accuracy and capability of the solution; all circuits required for programming are addressed and included in this benchmark.

The target frequency is the highest of all possible frequencies, although the filter needs to also operate with  $10 \times 100 \times 1000 \times 100$ 

# 3.5 Analog Computation Design Pushed through Simultaneous Benchmarks

These benchmarks simultaneously push different characteristics important for reconfigurable computational analog design as well as the tools for synthesizing a range of analog designs (Figure 11). Many opportunities are possible with existing SoC FPAA devices (350 nm CMOS), and yet, each benchmark problem shows particular design choices in an architecture exploration process. All four benchmarks must be satisfied by a particular configurable system or synthesis tool, each at

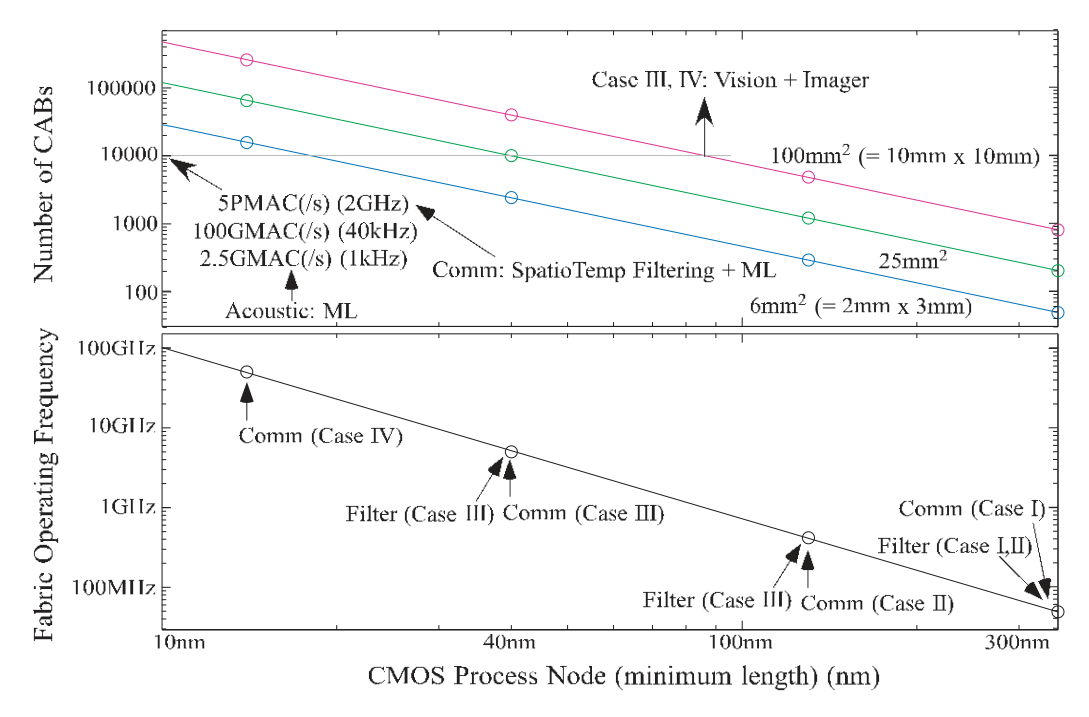


Fig. 11. Tradeoffs between FPAA implementations and benchmark problems for particular cases (Case I through Case IV). *Upper Graph*: Complexity for  $2 \times 3 \text{ mm}^2$ ,  $5 \times 5 \text{ mm}^2$ , and  $10 \times 10 \text{ mm}^2$  die sizes as a function of process node, calling out the 350 nm, 130 nm, 40 nm, and 14 nm CMOS nodes. Fabric operating frequency *Lower Graph*: Fabric operating frequency (frequency to near DC) as a function of process node, calling out the 350 nm, 130 nm, 40 nm, and 14 nm CMOS nodes.

their particular Case level. Custom designs will have some similar tradeoffs when targeted and will show design tool capabilities.

The *communication* benchmark primarily pushes the fabric frequency limitation (Figure 11). The size of the spatio-temporal filter for Case IV is possible in one to four SoC FPAA devices, although the frequency limitations around 50–60 MHz limit this benchmark. The Case III frequency metric (2 GHz) and spatio-temporal filter complexity were already exceeded by a 2 mm × 3 mm, 40 nm CMOS FPAA [53]. The Case IV metric should be easily satisfied at the 14 nm CMOS node.

The *acoustic* benchmark is not limited by frequency (kHz, very easy for 350 nm CMOS and scaled down technologies), but measures enabling parallel, real-time ML resources at this operating frequency. The front-end

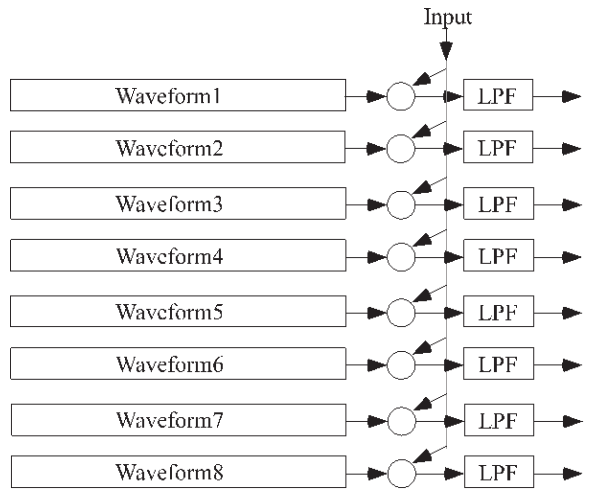


Fig. 12. Block diagram for an arbitrary waveform generation and following signal processing (e.g., modulation) functions.

12:14 J. Hasler and C. Hao

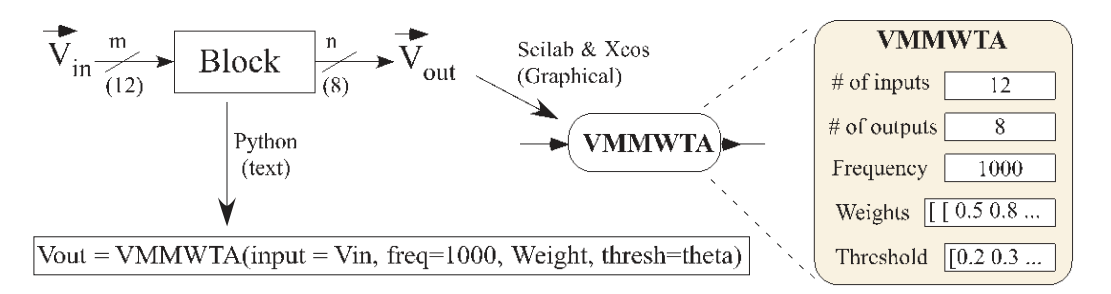


Fig. 13. An algorithm block is described by its computational function (physical devices), internal programmed parameters (e.g., FG values), and the signal busses of vectorized block inputs (e.g.,  $V_{in}$ ) and outputs (e.g.,  $V_{out}$ ). This block description is formulated in a graphics-based formulation (e.g., Xcos and Scilab) where the parameters are available graphically for each block, or are formulated in a text-based formulation that includes the parameters (e.g., Python routine syntax). Both formulations enable straightforward methods for macromodel simulations.

computation of 16 to 32 bands results in 16 to 32 CABs in the SoC FPAA with further optimizations expected in next-generation FPAA designs. The classifier (e.g., VMM+WTA) support in the SoC FPAA is 1 CAB per output symbol, although the next designs based on analog standard cells would routinely expect 8 to 16 symbol outputs per CAB. The issue is building an ML classifier (40 nm, 5 mm × 5 mm) with 2.5 M classifier parameters (e.g., Weights) running the very low-power ( $\mu$ W) 2.5 GMAC(/s) algorithm (Figure 11).

The *filter* benchmark is not limited by the number of CAB components, where this design is roughly 10 CABs of TA devices. This benchmark is limited by the fabric frequency, the quality of the circuits (linear range, power supply rejection), and the precision setting parameters. The SoC FPAA (350 nm) has suficient programming precision for these metrics. Case I (300 kHz) and potentially Case II (3 MHz) are possible in an SoC FPAA. Scaled CMOS nodes (Figure 11) should handle Case III (130 nm CMOS) and Case IV (40 nm CMOS).

The *imager* benchmark is limited by the CMOS imager choice and the number of parallel nodes for image computation. Local motion processing using 10,000 CABs enables a 16 × 16 image block within each CAB (3 MPixel imager), and in turn, enables a wide range of video/motion processing. With smaller networks, motion issues will be constrained by full-image storage. Case I and Case II focus on single image processing, while Case III and Case IV shift to motion/video processing corresponding to FPAA structures at 10,000 CAB level (Figure 11).

## 3.6 Additional Potential Benchmarks

This initial set of benchmarks can be expanded in the future to evaluate additional analog and mixed-signal computational aspects and likely will grow as computational algorithms grow (Figure 7). A potential set of future benchmark problems is briefly discussed in the following next paragraphs.

Generalized Linear and Nonlinear Dynamics: Analog computation enables a range of linear and nonlinear dynamics. The solution to A x = b problem through a differential equation  $\tau \frac{dx}{dt}$  enables the construction of linear control systems as well as certain potential nonlinear dynamical systems. These nonlinear dynamics could include optimization networks (e.g., Hopfield) or coupled chaotic systems. The ODEs in analog computation can be extended to PDEs that could be solved on configurable devices, including parabolic (e.g., diffusion/heat equation) or hyperbolic (e.g., wave propagation) equations. These techniques show significant numerical advantages for analog computation, as digital approaches require solving A x = b with a quadratically increasing condition number [70].

ACM Transactions on Reconfigurable Technology and Systems, Vol. 17, No. 1, Article 12. Pub. date: January 2024.

Neuron Modeling and Neuromorphic Computation: These directions are an important emerging application space (e.g., [90]) which are beyond discussions of VMMs, general ODE solutions, and solutions of linear equations, but rather are focused on the further improvement of neural algorithms toward engineering problems *beyond* the capability of analog computation [90]. Traditional easy models of rate-encoded signals and integrate and fire neurons are not the desired model in these areas (e.g., [90]). The uncertain nature of these emerging computations makes defining benchmarks in this area premature, although certainly, they will arise with continued research.

Signal Generation and Computation: Many computations (analog or digital) require the generation of parallel arbitrary signals that are multiplied with one or multiple signals (Figure 12). These techniques have multiple communication applications (e.g., OFDM, synchronized matched filters, security keys) that require arbitrary waveform generators with modulators and filters. Analog approaches can utilize dense memory elements where each stored analog value can be played in sequence (e.g., [31, 91, 92]).

#### 4 ANALOG ALGORITHMS ENABLING ANALOG BENCHMARKS

Between the Benchmarks and the configurable FPAA devices is the analog algorithm representation. The benchmark problems set some of the user-facing algorithm blocks that aggregate to benchmark solutions, enabling a top-down design methodology for analog computation similar to digital computational flows. These algorithm blocks make analog system design accessible to digital algorithm designers. A designer only needs to understand a few additional concepts but not the whole field of analog circuit design. These abstractable blocks, similar to digital computation, are effectively considered recognizable computations. These algorithm definitions provide a set of user-facing algorithms abstracting analog computation from most users. A coding framework enables some level of benchmark portability, although the number of options for implementation is small at the writing of this article (e.g., FPAAs, early synthesis); we expect that further tool development can accelerate these opportunities and widen the use of these concepts. These algorithmic functions transform the expected lived experience of analog design.

algorithm An block can be represented either as a text representation (e.g., a Python function call) or as a graphical representation (e.g., Xcos) block where the parameters can be selected through the graphical interface (Figure 13). the algorithm blocks are vector-(buses

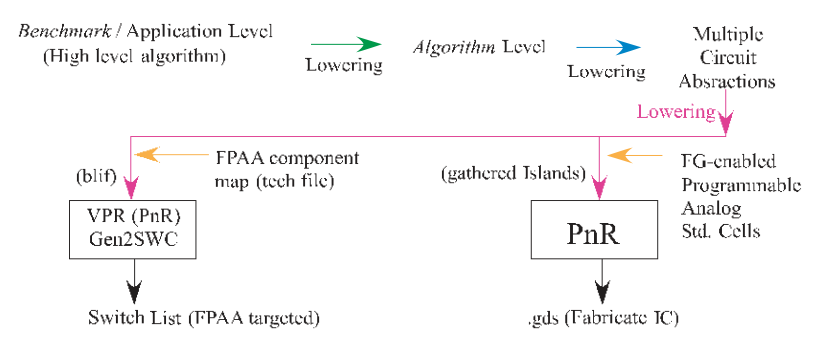


Fig. 14. Benchmark or Application level and Algorithm level within a high-level perspective of a programmable analog synthesis tool flow either to target an FPAA or to create the design for a new IC.

abstracted, Figure 6) level = 1 (Figure 4) blocks with the expected vectorization that can have a Python-level definition. Graphical blocks illustrate the computation dataflow (level = 1), although the text-based formulation (Python functions) is functionally equivalent (Figure 13)). Each block should have a macromodel for potential digital simulation. Traditional circuit design for developing new algorithm blocks (level = 1) is enabled through separate level = 2 current-voltage

12:16 J. Hasler and C. Hao

representations and simulation, where eventually a resulting level = 1 block is defined and macromodelled. Analog circuit design becomes complete when a circuit design is abstracted into a tool f low.

The Benchmark application is instantiated into a sequence of algorithm-level blocks specified either as a graphical or text framework. Graphical compilation from Xcos/Scilab graphical representation (Figure 13) to targeted FPAA code [57, 61, 93] is a process utilized by multiple research groups. Recent efforts have developed a generalized synthesis tool flow (Figure 14) from Python to Verilog to Netlist to a switch list (targetable FPAA file) through an FPAA description file as well as to IC layout (.gds) through programmable analog standard cells [62, 63]. Algorithm blocks enable the infrastructure for multiple levels of architectural exploration for developing new configurable systems (e.g., for digital: OpenFPGA [94]) enabling high-level (algorithm simulation) and lower-level (device simulation) comparisons.

The range of level = 1 algorithm computation (Figure 15) includes programmable first- and second-order LPF and BPFs, a range of VMM-enabled computations, nonlinear dynamics, and utility functions. These blocks have been implemented often on existing FPAAs (Figure 18), including in the SoC FPAA. Each function has system parameters and circuit parameters, where the system parameters can be lowered to the circuit parameters. The LPF includes HopfLPF second-order block with programmable nonlinear dynamics and Ladder filter (LadderF, LadderFM) stages used for filters, delay stages, as well as computation for this effective 1-D space, 1-D time second-order PDE. The BPF includes adaptive BPF elements (AdaptBPF) as well as elements that perform a tunable amplitude detection after the BPF (AmplitudeBPF, AmplitudeAdaptBPF). A BPF element will have system parameters (parameter vectors centerFreq, Q) that directly set programmable circuit biases (parameter vectors Ibias1, Ibias2) for TA through other circuit parameters (e.g., load capacitances). As a VMM operation typically has voltage-in and current-out of the crossbar, such a computation is not a level = 1 operation [45, 59], requiring either a merge with the next level of computation (e.g., WTA: VMMWTA, sigmoid for NN: SigVMM) or a current-to-voltage (e.g., a transimpedance am-plifier) to create voltage outputs. The freq parameter specifies the maximum operating frequency and enables tools to convert the system parameters (W) to circuit parameters (Ibias) through the circuit components (e.g., capacitance). A range of linear and nonlinear dynamics are available through more advanced blocks, such as the linear equation solution (Linear EqIterate) that also enables creating a linear system definition for control systems, the Hodgkin-Huxley (HH) Neu-ron and synapses (NeuronHH), or using the SigVMM block to build Hopfield recurrent dynamics. Several computation utilities (e.g., M2V = Matrix to Vector transformation) enable reformatting the data where required. The blocks are not an exhaustive list but are highly representative of cur-rently defined functions (Figure 15(a)); additional algorithm blocks are expected moving forward. The physical implementation involves a range of CAB/CLB utilization depending on the particular FPAA device (e.g., SoC FPAA, Figure 18) as well as various areas depending on the programmable analog standard cell library available (e.g., [63]).

The algorithm blocks can fully specify solutions for the four benchmark problems. The *vision benchmark* primarily uses the imager convolution algorithm, ImageVMM(), which performs a separable image transform. Commercial imagers communicate a single sample at a time by scanning the entire image sensor array. The imaging architecture should utilize this data format as much as possible to minimize the communication cost (e.g., [33, 74]). The first stage of these algorithms is a set of 2-D separable transforms with a WTA block enabling the first layer of classification. The resulting layers of transforms, classification, and compression reduce the image into a vector

<sup>&</sup>lt;sup>3</sup>the synthesis flow to an FPAA or to a custom layout from these Python definitions is currently under review and will be made available when they are accepted.

Lowpass Filters  LPF( ) HopfLPF( )  LadderF( )  LadderFM( )	Bandpass Filters  BPF( ) AmpliltudeBPF( )  AdaptBPF( )  AmplitudeAdaptBPF( )	Dynamics Blocks LinearEqIterate( ) NeuronHH( )
VMM Blocks VMMWTA( ) VMM( ) SigVMM( ) VMMDemod( )	2-D Blocks LocalSepImagerConv( ) ClassifyBlockIage2Vector( )	Utilities Scanner( ) M2V( ) MergeV( )

			(a)			
Function Area	Function	Input	Output	System Parameters	Circuit Parameters	
Lowpass	LPF	n	n	cornerFreq(n)	Ibias(n)	
Filters:	HopiLPF	1	n	centerFreq(n), Q(n)	Ibias1(n), Ibias2(n)	
	LadderF	1	n	delay(n)	Ibias1(n), Ibias2(n)	
	LadderFM	m	$n \times m$	delay(n)	Ibias1(n), Ibias2(n)	
Bandpass:	BPF	1	n	centerFreq(n), Q(n)	Ibias1(n), Ibias2(n)	
Filters:	AdaptBPF	1	n	centerFreq(n), Q(n)	Ibias(n), Iq(n)	
	AmplitudeBPF	1	n	centerFreq(n), Q(n), AmpDetect(n)	Ibias1(n), Ibias2(n), Ibias $\Lambda$ (n)	
	AmplitudeAdaptBPF	1	n	centerFreq(n), Q(n), AmpDetect(n)	Ibias(n), Iq(n), IbiasA(n)	
VMM:	VMM	m	n	W(m×n), freq(1)	Ibias(n×m)	
blocks	VMMWTA	m	n	W(m×n), Thresh(n), freq(1)	Ibias(n $\times$ m), Ithresh(n)	
	SigVMM	m	n	W(m×n), freq(1)	Ibias(n×m)	
	VMMDemod	m+1	n	W(m×n), mod(1), freq1(1), freq2(1)	Ibias(n $\times$ m), Ibias2(n)	
Dynamics	LinearEqllerate	n	n	$\Lambda(n \times n)$ , $b(n)$ , freq(1)	Ibias∆(n×n), IbiasB(n)	
Blocks	NeuronHH	m	n	W(m×n)	Isyn(m×n)	
2-D Blocks	LocalSepImagerConv	1	m	vert=V1, horiz=h1,clock	Ivert, Ihoriz, clock	
	ClassifyBlockImage2Vector	m	n	clock,	clock	
Utilities	Scanner	m+2	1	clock(1), data(1)		
	M2V	$m \times n$	m n			
	MergeV	m, n	m+n			
			(b)			

Fig. 15. A partial list of algorithm functions for implementing benchmarks. (a) Several functions gather into multiple function areas. (b) Greater detail on the algorithm (.py) level = 1 function definitions. Each of these blocks would have a parallel definition for the highest level in Verilog-AMS with the same names. In addition to these *signal* values, there are a number of parameter values for each function.

Sample Acoustic Benchmark Code	Sample Vision Benchmark Code			
y1 = AmplitudeBPF(In, center=f1, Q=Q1, fpeak = f2)	y1 = LocalSepImagerConv(input=In,vert=V1,horiz=h1,clock=CK1)			
y2 = M2V( LadderFM(input=y1,lbias1=Ib1,lbias2=Ib2) )	y2 = ClassifyBlockImage2Vector(input=y1, ,clock=CK1)			
Out = VMMWTA(input=y2,W=W1,Thresh=theta1,freq=400)	Out = VMMWTA (input = y2, W = Wimage, Thresh = theta2, freq = 60)			
Sample Analog Benchmark Code	Sample Communication Benchmark Code  y1 = LadderF(input=In,Ibias1=If1,Ibias2=If2)  y2 = VMMDemod(input=y1,W=W1, mod=Signal1, freq1=2.5e9, freq2=1e			
<u> </u>				
y1 = LadderF(input=In,Ibias1=If1,Ibias2=If2)				
Out = yl(n)	Out = VMMWTA(input=y2,W=W1,Thresh=theta3,freq=1e7)			

Fig. 16. Example Code Blocks for four benchmarks using analog algorithms, including a sample Acoustic, Vision, Communication, and Analog Benchmark Code. These blocks include the parameters as well as the computational flow.

metric, enabling a VMM+WTA classifier for the measured result. For the communication benchmark for a single input (all are defined for multiple inputs, so using LadderFM instead of LadderF), y1 is a vector (e.g., qw) corresponding to Ibias1 and Ibias2 creating delays along the line. These

12:18 J. Hasler and C. Hao

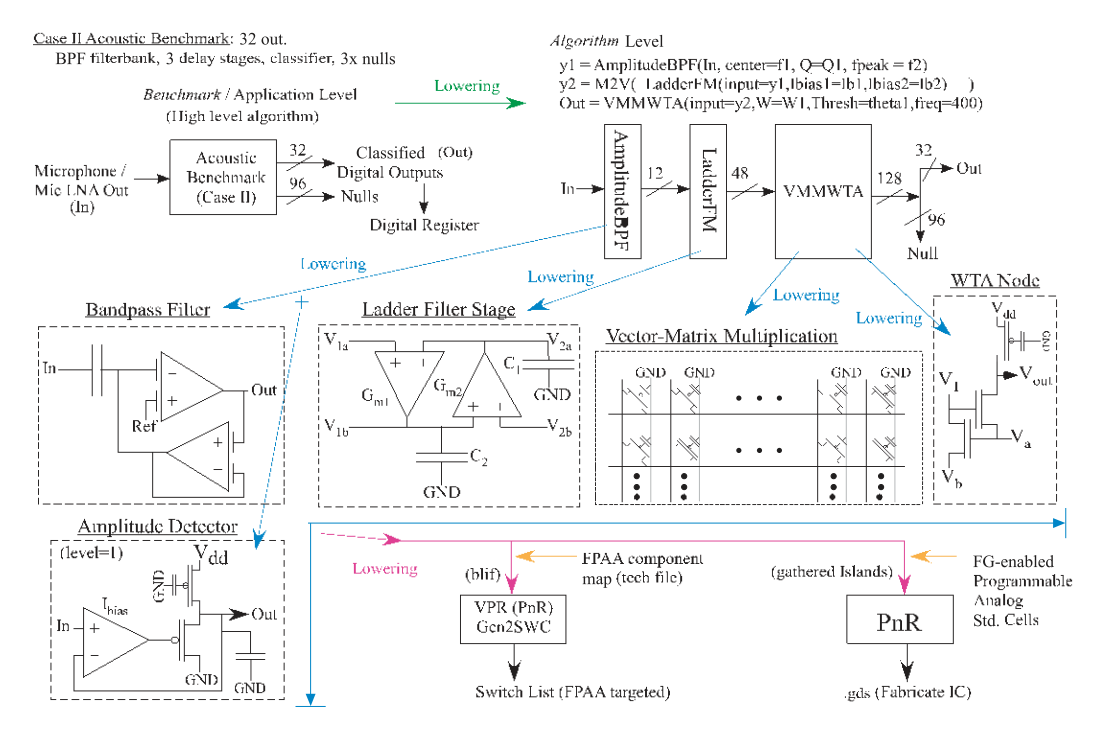


Fig. 17. Benchmark level lowering to Algorithmic Level example for an acoustic Case II implementation, classifying 32 command words from a microphone signal. This implementation uses 96 nulls, classified outputs that are not the desired 32 command words, for increased system robustness, typical of other speech recognition systems. Another user could choose to solve this benchmark application through other architectures. Most commercially available microphones already contain a Low-Noise Amplifier (LNA), therefore, the input sensor signal would come after this stage. This benchmark solution is composed of multiple algorithm-level functions, with the resulting intermediate scalar (freq), vector (Ibias1, Ibias2, theta), and matrix (W) parameters required for each stage. The flow illustrates the tool synthesis to either target an FPAA or fabricate a new IC, including lowering the AmpitudeBPF block into its component (level = 1) Bandpass Filter and Amplitude Detector block circuits, lowering the LadderFM block into its component Ladder Filter Stages, and lowering the VMMWTA block into the crossbar VMM, often implemented in routing fabric, and WTA node circuits.

spatio-temporal beamforming (VMM) are input into a parallel demodulation system (e.g., 32) and are passed to a classifier to generate multiple classified output signal lines in a vector (e.g., 64). This system also requires a demodulation signal (Signal1) that is an input modulation signal in the 2 to 2.5 GHz range. One can specify that all of the four benchmark cases (defined) have only a single analog input (In). The imager input could be analog or digital, but given it is one signal, a single DAC can handle the conversion, so we will consider all of the questions with a single scalar signal input (In). The analog benchmark would have multiple of these parallel filters.

A high-level implementation example of one benchmark, the acoustic Case II benchmark, illustrates the steps starting from the benchmark instantiate in the algorithm code, and the lowering and compilation strategy (Figure 17). The Python description gets lowered into Verilog AMS and through the resulting tools to a switch list or a .gds output. For the Case II acoustic benchmark (Figure 17), for single microphone input, y1 is an output vector corresponding to the output feedback vector (12 lines), y2 is an output vector corresponding to three approximate delays at each BPF stage set through Ibias1 (e.g., 3 by 12) and Ibias2 (e.g., 3 by 12) creating delays (48 lines), and a

			Previous
Function Area	Function	Size	Measure
Lowpass	LPF	1/4 CAB (TA)	[31]
Filters:	HopfLPF	1 CAB (4 TA)	[86]
	LadderF	1 CAB / stage (2FG TA)	[75]
	LadderFM		[75]
Bandpass:	BPF	1/2 CAB (2 TA)	[31]
Filters:	AdaptBPF	3/4 CAB (3 TA)	[95]
	AmplitudeBPF	1 CAB (4 TA)	[31, 96]
	AmplitudeAdaptBPF	1 CAB (4 TA)	(internal)
VMM:	VMM	R + 4TA (13in + 2 out/CAB)	[97]
blocks	VMMWTA	$\mathbf{R}$ + 2nFETs (13in + 1 out/CAB)	[73, 80, 98]
	SigVMM	$\mathbf{R} + 4  \text{tA}  (13 \text{in} + 4  \text{out/CAB})$	[99]
	VMMDemod		(internal)
Dynamics	LinearEqIterate	4 Matrix elements / CAB	[100]
Blocks	NeuronHH	$\mathbf{R}$ + CAB (13in + 1 out/CAB)	[101]
2-D Blocks	LocalSepImagerConv		[33]
	ClassifyBlockImage2Vector		[33, 74]
Utilities	Scanner	1 16bit shift reg / CAB	[92]
	M2V	$m\times n$	(typical)
	MergeV		(typical)

Fig. 18. FPAA sizes for the partial list of algorithm (.py) function definitions at level = 1. The FPAA sizes are baselined to the CABs in the SoC FPAA [31]. Previous CAB components were designed by intuition as most system infrastructure was not available. New CABs and new FPAA architectures and designs will be optimized utilizing benchmarks. Many functions utilize the CAB Routing (R for the computation. Some internal functions have not yet been published at this stage.

48-input by 128-output VMM+WTA classifier stage with a 6,144 weight matrix. This system would require more WTA stages than would fit on an SoC FPAA (barely), although such a design could theoretically be implemented on two SoC FPAAs (350 nm CMOS), and potentially easily implemented in a similar size 130 nm FPAA. Using 130 nm standard cells, this implementation would roughly require an area of 250  $\mu$ m × 300  $\mu$ m. Functions can have parameters at a higher function level, such as frequency or weights, or lowered values such as bias currents. Our synthesis tools lower functionality from higher level to lower level parameters. This example explicitly shows both cases.

### 5 ANALOG AND MIXED-SIGNAL SUMMARY AND DISCUSSION

This first analog and mixed-signal benchmark suite of various sizes and domains enables performance evaluation and optimization with recent analog and mixed-signal design and synthesis tools. These benchmarks comprise multiple levels of an acoustic system, a vision system, a communications system, and a classical analog filter system that must be simultaneously satisfied for a complete system. ML is essential in two systems, and can be utilized in the other two systems. Defining the analog computation system benchmark and its underlying computation enables future automated architectural DSE, to determine the best configurable architecture (e.g., a new FPAA) for a certain family of applications. The demonstration of the benchmarks will further show the 1,000 × improvement (and more) that Mead originally discussed (1990) [46] and illustrate further ways to utilize these concepts.

12:20 J. Hasler and C. Hao

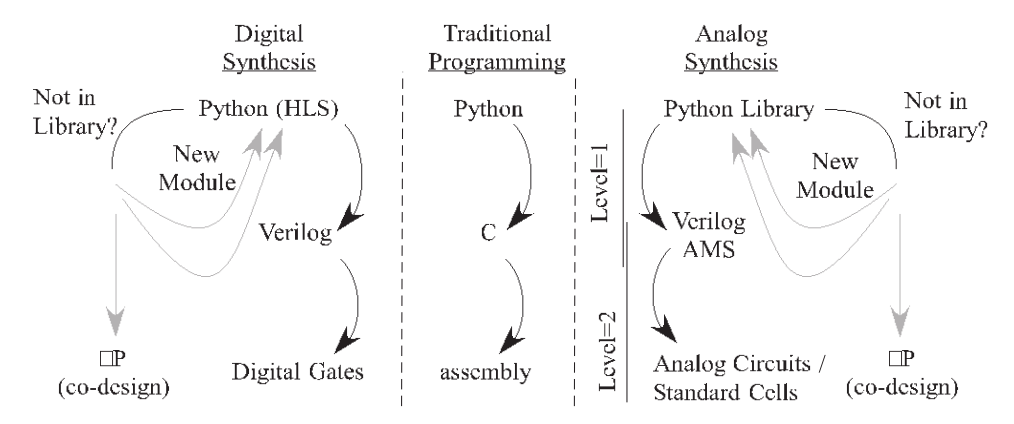


Fig. 19. Similar to traditional programming which has a hierarchy and compilation flow from higher-level languages (e.g., Python) to more machine-specific languages (e.g., C and assembly), digital and analog synthesis for configurable structures has similar flows. If a component is not in the library so that the tools cannot directly compile a block, it opens an opportunity for the design of a new module in a lower tool flow and/or direct compilation of that block into a processor co-designed with the implementation.

Benchmarks are an indicator of the perceived fundamental computations of that particular computing substrate. Although digital computing benchmarks mostly follow the solution of linear equations, analog benchmarks utilize ODE, PDE, and some linear equation solutions. These efforts enable the evaluation of targeted FPAAs, custom ICs, and new FPAA designs through recent analog computing theory. Abstracting the capabilities of analog computing shows the resulting analog benchmarks. These benchmarks are composed of an initial set of analog and mixed-signal algorithm blocks that provide solutions for these particular benchmarks.

One expects analog synthesis tools to eventually parallel digital and coding synthesis tools, including enabling adding new functionalities to the libraries at different levels (Figure 19). The lower-level tools exist to handle functions or features that are not currently in the algorithm library (Figure 19). Tools enable building blocks with the full analog circuit capability (e.g., level = 2, [60]) that build up to new level = 1 blocks as well as enabling expert designers to utilize more device-level features. A digital programmer (Figure 19) might utilize a similar flow utilizing C code or even assembly code in a larger Python project, or an FPGA designer might utilize Verilog or gate-level design in a C++

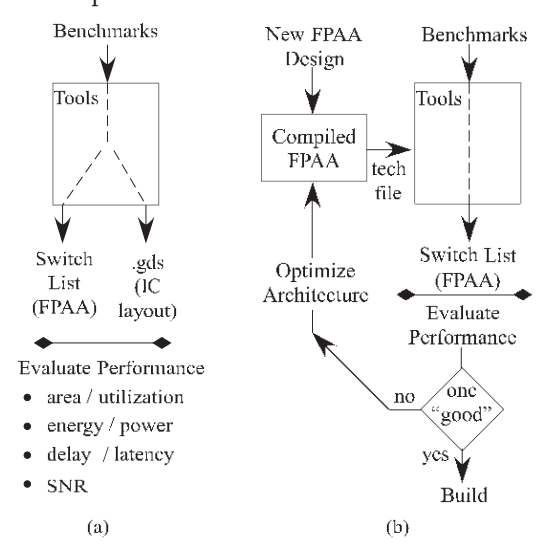


Fig. 20. Potential benchmark applications for application synthesis. (a) Benchmarks enable the evaluation of analog tool synthesis to either an FPAA or a new analog IC. (b) Benchmarks enable the design of new FPAAs by enabling tool synthesis, evaluation, and redesign.

or Python-defined project. If an  $\exp(\cdot)$  or  $\sin(\cdot)$  function is not available for an FPGA or embedded design, it could be built at a lower level and incorporated into the function library. The capability is similar to analog computation and synthesis.

Benchmarks provide new FPAA devices metrics (e.g., scaled FPAA technologies), enabling optimizing synthesis procedures through analog-digital co-design space exploration (Figure 20). An automated architectural DSE can determine the best architecture (e.g., a new FPAA) compared to these benchmarks, adapting the compiled FPAA technology files for scaled FPAA devices (Figure 20). The performance evaluation includes area and resource allocation, energy and power, SNR, and delay and latency. Some metrics can be directly evaluated by the synthesis procedure, while others require a level of circuit and system simulation to verify the synthesized performance. Benchmarking evaluates the proposed automation tool as well as the generated analog/mixed-signal circuit or device (Figure 20).

The mixture of potential analog computation, digital computation, and specialized digital components (e.g., a  $\mu$ P) creates the analog-digital hardware-software co-design problem, a problem that system performance against the benchmark suite will give some intuition for particular systems designs. When should an algorithm, or part of an algorithm, be performed on a  $\mu$ P, in digital fabric, and in analog fabric? For low-power computation, numerically intense computations can shift to analog components, and the processor can address the control flow and movement of data streams throughout the computation. Some functions will be explicitly specified by the designer, whereas some functions will have characterized options for both digital and analog options. Some tool flows can be easily compiled from known routines, whereas some may require more complex synthesis requiring designer interaction to utilize designers' expertise in the optimization. The question of choosing a particular resource for a function will require building a performance estimation model, including the algorithmic and architecture complexity of the analog and digital components, where the performance of various options is evaluated against the defined benchmarks.

#### REFERENCES

- [1] J. J. Dongarra, P. Luszczek, and A. Petitet. 2003. The LINPACK benchmark: Past, present and future. Concurrency Computation Practice and Experience (2003), 803–820.
- [2] J. Hasler. 2017. Starting framework for analog numerical analysis for energy efficient computing. Journal of Low Power Electronics Applications 7, 17 (2017), 1–22.
- [3] Yuko Hara, Hiroyuki Tomiyama, Shinya Honda, Hiroaki Takada, and Katsuya Ishii. 2008. CHStone: A benchmark program suite for practical c-based high-level synthesis. In Proceedings of the 2008 IEEE International Symposium on Circuits and Systems (ISCAS). 1192–1195.
- [4] Chunho Lee, Miodrag Potkonjak, and William H. Mangione-Smith. 1997. Mediabench: A tool for evaluating and synthesizing multimedia and communications systems. In Proceedings of the 30th Annual International Symposium on Microarchitecture. IEEE, 330–335.
- [5] Brandon Reagen, Robert Adolf, Yakun Sophia Shao, Gu-Yeon Wei, and David Brooks. 2014. Machsuite: Benchmarks for accelerator design and customized architectures. In Proceedings of the 2014 IEEE International Symposium on Workload Characterization (IISWC). IEEE, 110–119.
- [6] Sven Verdoolaege, Juan Carlos Juega, Albert Cohen, Jose Ignacio Gomez, Christian Tenllado, and Francky Catthoor. 2013. Polyhedral parallel code generation for CUDA. ACM Transactions on Architecture and Code Optimization 9, 4 (2013), 1–23.
- [7] Yuan Zhou, Udit Gupta, Steve Dai, Ritchie Zhao, Nitish Srivastava, Hanchen Jin, Joseph Featherston, Yi-Hsiang Lai, Gai Liu, Gustavo Angarita Velasquez, Wenping Wang, and Zhiru Zhang. 2018. Rosetta: A realistic high-level synthesis benchmark suite for software programmable FPGAs. In *Proceedings of the FPGA*.
- [8] Aman Arora, Andrew Boutros, Daniel Rauch, Aishwarya Rajen, Aatman Borda, Seyed Alireza Damghani, Samidh Mehta, Sangram Kate, Pragnesh Patel, Kenneth B. Kent, Vaughn Betz, and Lizy K. John. 2021. Koios: A deep learning benchmark suite for FPGA architecture and CAD research. In *Proceedings of the FPL*.
- [9] Dirk Stroobandt, Peter Verplaetse, and Jan Van Campenhout. 2000. Generating synthetic benchmark circuits for evaluating CAD tools. IEEE Transactions on Computer-Aided Design of Integrated Circuits and Systems 19, 9 (2000), 1011–1022.

12:22 J. Hasler and C. Hao

[10] Geoffrey Ndu, Javier Navaridas, and Mikel Luján. 2015. CHO: Towards a benchmark suite for OpenCL FPGA accelerators. In Proceedings of the 3rd International Workshop on OpenCL. 1–10.

- [11] Shuai Che, Michael Boyer, Jiayuan Meng, David Tarjan, Jeremy W. Sheaffer, Sang-Ha Lee, and Kevin Skadron. 2009. Rodinia: A benchmark suite for heterogeneous computing. In Proceedings of the 2009 IEEE International Symposium on Workload Characterization (IISWC). Ieee, 44–54.
- [12] Konstantinos Krommydas, Wu-chun Feng, Christos D. Antonopoulos, and Nikolaos Bellas. 2016. Opendwarfs: Characterization of dwarf-based benchmarks on fixed and reconfigurable architectures. *Journal of Signal Processing Systems* 85 (2016), 373–392.
- [13] Anthony Danalis, Gabriel Marin, Collin McCurdy, Jeremy S. Meredith, Philip C. Roth, Kyle Spafford, Vinod Tipparaju, and Jeffrey S. Vetter. 2010. The scalable heterogeneous computing (SHOC) benchmark suite. In Proceedings of the 3rd Workshop on General-purpose Computation on Graphics Processing Units. 63–74.
- [14] Quentin Gautier, Alric Althoff, Pingfan Meng, and Ryan Kastner. 2016. Spector: An OpenCL FPGA benchmark suite. In *Proceedings of the 2016 International Conference on Field-Programmable Technology (FPT)*. IEEE, 141–148.
- [15] Raphael Njuguna and Raj Jain. 2008. A survey of FPGA benchmarks. Project Report, November 24 (2008).
- [16] Matthew R. Guthaus, Jeffrey S. Ringenberg, Dan Ernst, Todd M. Austin, Trevor Mudge, and Richard B. Brown. 2001. MiBench: A free, commercially representative embedded benchmark suite. In Proceedings of the 4th Annual IEEE International Workshop on Workload Characterization. WWC-4 (Cat. No. 01EX538). IEEE, 3–14.
- [17] Andrew Canis, Jongsok Choi, Mark Aldham, Victor Zhang, Ahmed Kammoona, Jason H. Anderson, Stephen Brown, and Tomasz Czajkowski. 2011. LegUp: High-level synthesis for FPGA-based processor/accelerator systems. In Proceedings of the 19th ACM/SIGDA International Symposium on Field Programmable Gate Arrays. 33–36.
- [18] Rehan Ahmed, Assem A. M. Bsoul, Steven J. E. Wilton, Peter Hallschmid, and Richard Klukas. 2014. High-level synthesis-based design methodology for dynamic power-gated FPGAs. In Proceedings of the 2014 24th International Conference on Field Programmable Logic and Applications (FPL). 1–4. DOI:http://dx.doi.org/10.1109/FPL.2014.6927433
- [19] Vitis High-Level Synthesis. Retrieved from https://www.xilinx.com/products/design-tools/vivado/integration/esl-design.html. Accessed September 14, 2023.
- [20] CIRCT Project under MLIR Framework. Retrieved from https://circt.llvm.org/. Accessed September 14, 2023.
- [21] Sitao Huang, Kun Wu, Hyunmin Jeong, Chengyue Wang, Deming Chen, and Wen-mei Hwu. 2021. Pylog: An algorithm-centric python-based FPGA programming and synthesis flow. In Proceedings of the 2021 ACM/SIGDA International Symposium on Field-Programmable Gate Arrays. 227–228.
- [22] Hanchen Ye, Cong Hao, Hyunmin Jeong, Jack Huang, and Deming Chen. 2021. ScaleHLS: Achieving scalable high-level synthesis through MLIR. *LATTE Workshop on Languages, Tools, and Techniques for Accelerator Design* (2021).
- [23] Daniel W. Chang, Christipher D. Jenkins, Philip C. Garcia, Syed Z. Gilani, Paula Aguilera, Aishwarya Nagarajan, Michael J. Anderson, Matthew A. Kenny, Sean M. Bauer, and Michael J. Schulte. 2010. ERCBench: An open-source benchmark suite for embedded and reconfigurable computing. In Proceedings of the 2010 International Conference on Field Programmable Logic and Applications. IEEE, 408–413.
- [24] Luca Amarú, Pierre-Emmanuel Gaillardon, and Giovanni De Micheli. 2015. The EPFL combinational benchmark suite. In Proceedings of the 24th International Workshop on Logic and Synthesis (IWLS).
- [25] V. Betz. The FPGA Place-and-Route Challenge. Retrieved from http://www.eecg.toronto.edu/~vaughn/challenge/challenge.html. Accessed September 14, 2023.
- [26] Wolf. 1994. Hardware-software co-design of embedded systems. Proceedings of the IEEE (1994), 967-989.
- [27] Q. Zhao, M. Amagasaki, M. Iida, M. Kuga, and T. Sueyoshi. 2013. An automatic FPGA design and implementation framework. In *Proceedings of the IEEE DAC*.
- [28] M. Weinhardt, A. Krieger, and T. Kinder. 2013. A framework for PC applications with portable and scalable FPGA accelerators. In *Proceedings of the IEEE DAC*.
- [29] D. Rossi, C. Mucci, M. Pizzotti, L. Perugini, R. Canegallo, and R. Guerrieri. 2014. Multicore signal processing platform with heterogeneous configurable hardware accelerators. *IEEE Transactions on VLSI* 22, 9 (2014), 1990–2003.
- [30] J. Hasler. 2020. Large-scale field programmable analog arrays. IEEE Proceedings 108, 8 (2020), 1283–1302.
- [31] S. George, S. Kim, S. Shah, J. Hasler, M. Collins, F. Adil, Wunderlich R, S. Nease, and S. Ramakrishnan. 2016. A programmable and configurable mixed-mode FPAA SoC. IEEE Transactions on VLSI 24, 6 (2016), 2253–2261.
- [32] J. Hasler, S. Kim, and A. Natarajan. 2018. Enabling energy-eficient physical computing through analog abstraction and IP reuse. *Journal of Low Power Electronics Applications* 8, 4 (2018), 1–23.
- [33] J. Hasler. 2019. Analog architecture and complexity theory to empowering ultra-low power configurable analog and mixed mode SoC systems. *Journal of Low Power Electronics Applications* 9, 1 (2019), 1–38.
- [34] J. Hasler and E. Black. 2021. Physical computing: Unifying real number computation to enable energy efficient computing. *Journal of Low-Power Electronics Applications* (2021), 1–21.
- [35] OpenMSP430 Project: Open Core MSP430. Retrieved from http://opencores.org/projectopenmsp430. Accessed September 14, 2023.

- [36] Jennifer Hasler. 2022. The potential of SoC FPAAs for emerging ultra-low-power machine learning. *Journal of Low Power Electronics and Applications* 12, 2 (2022).
- [37] Hasler, B. Minch, and C. Diorio. 1999. Adaptive circuits using pFET floating-gate device. In Proceedings of the Advanced Research in VLSI. 215–229.
- [38] M. Kucic, Hasler, J. Dugger, and D. Anderson. 2001. Programmable and adaptive analog filters using arrays of floating-gate circuits. In *Proceedings of the Advanced Research in VLSI*. 148–162.
- [39] T. Hall, D. Anderson, and Hasler. 2002. Field-programmable analog arrays: A floating-gate approach. In *Proceedings of the Field-Programmable Logic (FPL) and Applications*. Springer-Verlag, Montpellier, France, 424–433.
- [40] M. A. Brooke. 1988. A Reconfigurable General Purpose Analog Integrated Circuit. Ph.D. Dissertation. University Southern California.
- [41] M. A. Sivilotti. 1991. Wiring Considerations in Analog VLSI Systems, With Application to Field-Programmable Networks (VLSI). Ph.D., California Institute of Technology, Pasadena, CA.
- [42] E. K. F. Lee and P. G. Gulak. 1991. A CMOS field programmable analog array. IEEE JSSC (1991), 1860-1867.
- [43] H. W. Klein. 1992. The EPAC architecture: An expert cell approach to field programmable analog circuits. In Proceedings of the IEEE Midwest CAS. 169–172.
- [44] Anadigm. 2004. Specifically generic analog functions for FPAAs: Anadigm says. EE Times (2004).
- [45] C. Schlottmann and Hasler. 2011. A highly dense, low power, programmable analog vector-matrix multiplier: The FPAA implementation. *IEEE Journal on Emerging CAS* 1, 3 (2011), 403–411.
- [46] C. Mead. 1990. Neuromorphic electronic systems. Proceedings of the IEEE 78 (1990), 1629–1636.
- [47] V. Srinivasan, G. Serrano, C. Twigg, and Hasler. 2008. Floating-gate-based programmable CMOS reference. IEEE Transactions CAS I 55, 11 (2008), 3448–3456.
- [48] S. Shah, H. Toreyin, J. Hasler, and A. Natarajan. 2017. Models and techniques for temperature robust systems on a reconfigurable platform. *Journal of Low Power Electronics Applications* 7, 21 (2017), 1–14.
- [49] S. Y. Peng, G. Gurun, C. M. Twigg, M. S. Qureshi, A. Basu, S. Brink, Hasler, and Degertekin F. L. 2009. A large-scale reconfigurable smart sensory chip. In *Proceedings of the IEEE ISCAS*. 2145–2148.
- [50] M. Laiho, J. Hasler, J. Zhou, C. Du, W. Lu, E. Lehtonen, and J. H. Poikonen. 2014. FPAA/Memristor hybrid computing infrastructure. IEEE Transactions CAS I (2014).
- [51] C. Twigg, J. Gray, and Hasler. 2007. Programmable floating-gate FPAA switches are not dead weight. In Proceedings of the IEEE ISCAS. 169–72.
- [52] V. Srinivasan, G. J. Serrano, J. Gray, and P. Hasler. 2007. A precision CMOS amplifier using floating-gate transistors for offset cancellation. *IEEE JSSC* 42, 2 (2007), 280–291.
- [53] J. Hasler and H. Wang. 2015. A fine-grain FPAA fabric for RF + Baseband. In Proceedings of the GOMAC.
- [54] S. Kim, J. Hasler, and S. George. 2016. Integrated floating-gate programming environment for system-level ICs. IEEE Transactions VLSI 24, 6 (2016), 2244–2252.
- [55] J. Hasler and S. Shah. 2018. Security implications for ultra-low power configurable analog and mixed mode SoC systems. Journal of Low Power Electronics and Applications (2018), 1–17.
- [56] J. Hasler, S. Kim, and F. Adil. 2016. Scaling floating-gate devices predicting behavior for programmable and configurable circuits and systems. *Journal of Low Power Electronics Applications* (2016).
- [57] M. Collins, J. Hasler, and S. George. 2016. An open-source toolset enabling analog-digital software codesign. *Journal of Low Power Electronics Applications* 6, 1 (2016), 1–15.
- [58] C. R. Schlottmann, C. Petre, and P. E. Hasler. 2011. Simulink framework for design to and automated conversion on large-scale FPAA devices. *IEEE Transactions VLSI* (2011).
- [59] C. Schlottmann and J. Hasler. 2014. High-level modeling of analog computational elements for signal processing applications. IEEE Transactions VLSI 22, 9 (2014), 1945–1953.
- [60] A. Natarajan and J. Hasler. 2017. Modeling, simulation and implementation of circuit elements in an open-source tool set on the FPAA. Analog Integrated Circuits and Signal Processing 91, 1 (2017), 119–130.
- [61] J. Luu, J. Goeders, M. Wainberg, A. Somerville, T. Yu, K. Nasartschuk, M. Nasr, S. Wang, T. Liu, N. Ahmed, K. B. Kent, J. Anderson, J. Rose, and V. Betz. 2014. VTR 7.0: Next generation architecture and CAD system for FPGAs. In Proceedings of the IEEE ASIC Seminar. 6:1–6:30.
- [62] J. Hasler. 2021. Defining analog standard cell libraries for mixed-signal computing enabled through educational directions. In Proceedings of the IEEE ISCAS.
- [63] J. Hasler, B. Muldrey, and P. Hardy. 2021. A CMOS programmable analog standard cell library in skywater 130nm open-source process. In *Proceedings of the WOSET*.
- [64] Carver Mead and Lynn Conway. 1980. Introduction to VLSI System Design. Addison-Wesley. Retrieved from http://ai.eecs.umich.edu/people/conway/VLSI/VLSIText/VLSIText.html
- [65] G. E. Moore. 1965. Cramming more components onto integrated circuits. *Electronics* 38, 8 (1965).
- [66] G. E. Moore. 1975. Progress in digital integrated electronics. IEEE IEDM (1975), 11-13.

12:24 J. Hasler and C. Hao

[67] B. Hoeneisen and C. A. Mead. 1972. Fundamental limitations in microelectronics – I. MOS technology. Solid State Electronics 15, 7 (1972), 819–829.

- [68] R. Turing. 1937. On computable numbers. Proceedings of the London Mathematical Society (1937), 230-265.
- [69] R. Chawla, A. Bandyopadhyay, V. Srinivasan, and P. Hasler. 2004. A 531 nW/MHz, 128x32 current-mode programmable analog vector-matrix multiplier with over two decades of linearity. In Proceedings of the CICC. 651.
- [70] J. Hasler and A. Natarajan. 2021. Continuous-time, configurable analog linear system solutions with transconductance amplifiers. *IEEE Circuits and Systems I* 68, 2 (2021), 765–775.
- [71] Mike Demler. 2018. Mythic multiplies in a flash: Analog in-memory computing eliminates DRAM read/write cycles. The Linley Group (2018).
- [72] S. Brink, J. Hasler, and R. Wunderlich. 2014. Adaptive floating-gate circuit enabled large-scale FPAA. IEEE Transactions on Very Large Scale Integration Systems 22, 11 (2014), 2307–2315.
- [73] J. Hasler and S. Shah. 2018. SoC FPAA hardware implementation of a VMM+WTA embedded learning classifier. *IEEE Journal on Emerging CAS* 8, 1 (2018), 28–37.
- [74] Scott Koziol. 2013. Reconfigurable Analog Circuits for Autonomous Vehicles. Ph.D. Dissertation. Georgia Institute of Technology.
- [75] Jennifer Hasler and Sahil Shah. 2021. An SoC FPAA based programmable, ladder-filter based, linear-phase analog filter. *IEEE Transactions on Circuits and Systems I: Regular Papers* 68, 2 (2021), 592–602.
- [76] John S. Garofolo, L. Lamel, W. Fisher, J. Fiscus, D. Pallett, and N. Dahlgren. 1983. TIMIT acoustic-phonetic continuous speech corpus. In *Proceedings of the Linguistic Data Consortium*, *Philadelphia*. Retrieved from https://github.com/ philipperemy/timit
- [77] R. Gary Leonard and George R. Doddington. 1993. TI Digits Database. Retrieved from https://catalog.ldc.upenn.edu/docs/LDC93S10/tidigits.readme.html. Accessed September 14, 2023.
- [78] Pete Warden. 2018. Speech commands: A public dataset for single-word speech recognition. arXiv:1804.03209. Retrieved from https://arxiv.org/abs/1804.03209
- [79] Vassil Panayotov, Guoguo Chen, Daniel Povey, and Sanjeev Khudanpur. 2015. Librispeech: An ASR corpus based on public domain audio books. In Proceedings of the 2015 IEEE International Conference on Acoustics, Speech and Signal Processing (ICASSP). 5206–5210. DOI:http://dx.doi.org/10.1109/ICASSP.2015.7178964
- [80] S. Shah and J. Hasler. 2018. VMM + WTA embedded classifiers learning algorithm implementable on SoC FPAA devices. IEEE Journal on Emerging CAS 8, 1 (2018), 65–76.
- [81] L. Bottou, C. Cortes, J. S. Denker, H. Drucker, I. Guyon, L. D. Jackel, Y. LeCun, U. A. Muller, E. Sackinger, P. Simard, and V. Vapnik. 1994. Comparison of classifier methods: A case study in handwritten digit recognition. In Proceedings of the 12th IAPR International Conference on Pattern Recognition, Vol. 3 - Conference C: Signal Processing (Cat. No.94CH3440-5). DOI:http://dx.doi.org/10.1109/ICPR.1994.576879
- [82] Tsung-Yi Lin, Michael Maire, Serge Belongie, James Hays, Pietro Perona, Deva Ramanan, Piotr Dollár, and C. Lawrence Zitnick. 2014. Microsoft COCO: Common objects in context. In Proceedings of the Computer Vision—ECCV 2014. David Fleet, Tomas Pajdla, Bernt Schiele, and Tinne Tuytelaars (Eds.), Springer International Publishing, 740–755.
- [83] Kaiming He, Xiangyu Zhang, Shaoqing Ren, and Jian Sun. 2016. Deep residual learning for image recognition. In Proceedings of the 2016 IEEE Conference on Computer Vision and Pattern Recognition (CVPR). 770–778. DOI:http://dx.doi.org/10.1109/CVPR.2016.90
- [84] Qing-Yuan Jiang, Yi He, Gen Li, Lei Li Jian Lin, and Wu-Jun Li. 2019. SVD: A large-scale short video dataset for near-duplicate video retrieval. In *Proceedings of the International Conference on Computer Vision*.
- [85] Rakshith Rajashekar, Marco Di Renzo, K. V. S. Hari, and Lajos Hanzo. 2018. A beamforming-aided full-diversity scheme for low-altitude air-to-ground communication systems operating with limited feedback. *IEEE Transactions on Communications* 66, 12 (2018), 6602–6613. DOI:http://dx.doi.org/10.1109/TCOMM.2018.2864980
- [86] J. Hasler. 2022. A programmable on-chip Hopf bifurcation circuit. IEEE CAS I, on IEEE Xplore (2022).
- [87] Randall L. Geiger and Edgar Sánchez-Sinencio. 1985. Active filter design using operational transconductance amplifiers: A tutorial. *IEEE Circuits and Devices Magazine* 1 (1985), 20–32.
- [88] P. A. Allen and D. R. Holberg. 2002. CMOS Analog Circuit Design (2nd. ed.). Oxford University Press.
- [89] C. Cuypers, Yoong Voo, Mykhaylo Teplechuk, and J. I. Sewell. 2005. General synthesis of complex analogue filters. IEE Proceedings-Circuits, Devices and Systems 152 (2005), 7–15. DOI:http://dx.doi.org/10.1049/ip-cds:20040816
- [90] Jennifer Hasler and H. Bo Marr. 2013. Finding a roadmap to achieve large neuromorphic hardware systems. Frontiers in Neuroscience 7 (2013).
- [91] C. Schlottmann, S. Shapero, S. Nease, and Hasler. 2012. A digitally-enhanced reconfigurable analog platform for low-power signal processing. IEEE JSSC 47, 10 (2012), 2174–2184.
- [92] Jennifer Hasler and Sahil Shah. 2018. Security implications for ultra-low power configurable analog and mixed mode SoC systems. *Journal of Low Power Electronics and Applications* (2018), 1–17.

- [93] Sihwan Kim, Sahil Shah, Richard Wunderlich, and Jennifer Hasler. 2021. CAD synthesis tools for floating-gate SoC FPAAs. Design Automation for Embedded Systems (2021), 1–16.
- [94] Xifan Tang, Edouard Giacomin, Aurélien Alacchi, Baudouin Chauviere, and Pierre-Emmanuel Gaillardon. 2019.
  OpenFPGA: An opensource framework enabling rapid prototyping of customizable FPGAs. In Proceedings of the 2019 29th International Conference on Field Programmable Logic and Applications (FPL). 367–374.
- [95] Jennifer Hasler. 2023. A programmable adaptive-Q BPF circuit. Second Revision to IEEE CAS I (2023).
- [96] S. Shah and J. Hasler. 2017. Tuning of multiple parameters with a BIST system. Journal of Low Power Electronics Applications 64, 7 (2017), 1772–1780.
- [97] Aishwarya Nagarajan and Jennifer Hasler. 2020. Built-in self-test of vector matrix multipliers on a reconfigurable device. In *Proceedings of the IEEE ISCAS*.
- [98] S. Shah and J. Hasler. 2017. Low power speech detector on a FPAA. In Proceedings of the IEEE ISCAS.
- [99] Pranav Mathews and Jennifer Hasler. 2023. Physical computing for Hopfield networks on a reconfigurable analog IC. In *Proceedings of the IEEE ISCAS*.
- [100] Jennifer Hasler and Aishwarya Natarajan. 2021. Continuous-time, configurable analog linear system solutions with transconductance amplifiers. *IEEE Circuits and Systems I* 68, 2 (2021), 765–775.
- [101] Aishwarya Natarajan and Jennifer Hasler. 2019. Implementation of synapses with Hodgkin-Huxley neurons on the FPAA. In *Proceedings of the IEEE ISCAS*.

Received 14 February 2023; revised 21 August 2023; accepted 2 September 2023